ACS APPLIED NANO MATERIALS

Article

Cite This: ACS Appl. Nano Mater. 2020, 3, 409−417

www.acsanm.org

Hybrid J-Aggregate−Graphene Phototransistor

Ozan Yakar,[†] Osman Balci,[‡] Burkay Uzlu,[§,∥] Nahit Polat,[†] Ozan Ari,[⊥] Ilknur Tunc,[#] Coskun Kocabas,[¶] and Sinan Balci*[,†]

[†]Department of Photonics, Izmir Institute of Technology, 35430 Izmir, Turkey

[‡]Department of Physics, Bilkent University, 06800 Ankara, Turkey

[§]Advanced Microelectronic Center Aachen, AMO GmbH, Otto-Blumenthal-Strasse 25, 52074 Aachen, Germany

[∥]Chair of Electronic Devices, RWTH, Aachen University, 52074 Aachen, Germany

[⊥]ASELSAN Research Center, Ankara, Turkey

[#]Department of Mechanical Engineering, University of Turkish Aeronautical Association, 06790 Ankara, Turkey

[¶]School of Materials and National Graphene Institute, University of Manchester, Oxford Rd., Manchester M13 9PL, U.K.

Supporting Information

ABSTRACT: J-aggregates are fantastic self-assembled chromophores with a very narrow and extremely sharp absorbance band in the visible and near-infrared spectrum, and hence they have found many exciting applications in nonlinear optics, sensing, optical devices, photography, and lasing. In silver halide photography, for example, they have enormously improved the spectral sensitivity of photographic process due to their fast and coherent energy migration ability. On the other hand, graphene, consisting of single layer of carbon atoms forming a hexagonal lattice, has a very low absorption coefficient. Inspired by the fact that J-aggregates have carried the role to sense the incident light in silver halide photography, we would like to use J-aggregates to increase spectral sensitivity of graphene in the visible spectrum. Nevertheless, it has been an outstanding challenge to place isolated J-aggregate films on graphene to extensively study interaction between them. We herein noncovalently fabricate isolated J-aggregate thin films on graphene by using a thin film fabrication technique we termed here membrane casting (MC). MC significantly simplifies thin film formation of water-soluble substances on any surface via porous polymer membrane. Therefore, we reversibly modulate the Dirac point of graphene in the J-aggregate/graphene van der Waals (vdW) heterostructure and demonstrate an all-carbon phototransistor gated by visible light. Owing to the hole transfer from excited excitonic thin film to graphene layer, graphene is hole-doped. In addition, spectral and power responses of the all-carbon phototransistor have been measured by using a tunable laser in the visible spectrum. The first integration of J-aggregates with graphene in a transistor structure enables one to reversibly write and erase charge doping in graphene with visible light that paves the way for using J-aggregate/graphene vdW heterostructures in optoelectronic applications.

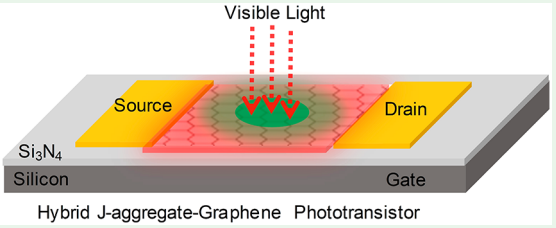

KEYWORDS: *J-aggregates, graphene, frenkel exciton, membrane casting, field effect transistor, phototransistor, dirac point, optoelectronics, photodetector*

INTRODUCTION

Graphene has received a tremendous amount of interest because of its exceptional electrical and optical properties[1,2] and has found many applications in the optoelectronics area such as solar cells,[3] light-emitting diodes, photodetectors,[4−6] lasers,[7] optical modulators,[8] and infrared camouflage.[9] Owing to its only 2.3% of light absorption, chemical and thermal stability, high flexibility, and one carbon atom thickness (0.345 nm), graphene has been used as a transparent conductor in photodetectors, solar cells, liquid crystal displays, field effect transistors, and light-emitting diodes in flexible and printable optoelectronics.[10−15] In addition, recently distict two-dimensional nanomaterials have been integrated with graphene into van der Waals (vdW) heterostructures.[16−18] In fact, most of these applications require controlling the type (n-type or p-type doping) and density of charge carriers on graphene.[19−22] To date, chemical doping,[19,23] electrostatic gating,[20,24] and photoinduced doping[25] have been frequently used to control charge density on graphene. Specifically, chemical doping is achieved by chemical compounds or nanoparticles near or in (substitutional doping) graphene,[23,26] electrical doping is obtained by changing the gate voltages,[22,27] and photoinduced doping is done by placing a light-sensitive chemical compound near graphene and by using light to excite that chemical compound.[25,28] Developing new ways of reversible and controllable doping (charge density and types) of graphene is urgently needed and very crucial for future graphene optoelectronics since increasing the level of doping in

Received: October 20, 2019
Accepted: December 11, 2019
Published: December 11, 2019

DOI: 10.1021/acsanm.9b02039
ACS Appl. Nano Mater. 2020, 3, 409−417

graphene will significantly modify optical properties of graphene; for example, high doping of graphene will extend graphene plasmon frequencies in the near-infrared region.[29]

In recent years, photoinduced doping has received a special interest because (I) photoinduced doping is a dynamic process where doping level of graphene can be reversibly controlled by light,[25,28] (II) high doping levels can be achieved ~10^{12} cm^{-2},[30] (III) current flow in the graphene transistor can be altered by light "light gating",[4] (IV) graphene-based photodetectors working in a broad range of wavelengths and good responsivity can be achieved,[4,5] and (V) p−n junctions can be optically and spatially created on graphene.[31] Until now, quantum dots,[4] light switchable azobenzene chromophores,[25,28] perovskites,[32,33] and two-dimensional nanomaterials[5,30] have been mainly used to efficiently photodope graphene with light. One of the most interesting and traditional light-sensitive supramolecular self-assembled structures is J-aggregates, first observed by Jelly and Scheibe in 1936,[34,35] which self-assemble at high concentration and show a very narrow and intense absorption band, which is shifted to longer wavelengths relative to the monomer absorption band. Notably, at high concentration, individual dye molecules organize in a brickstone work like structure, and thus J-aggregates can be considered as a two-dimensional system.[35−37] In fact, J-aggregates were popularly used for spectral sensitization of photographic processes with silver halides because of strong light absorption in the visible spectrum.[35] Likewise, inspired by the fact that J-aggregates have carried the role to sense the incident light in silver halide photography, we herein use J-aggregates to increase spectral sensitivity of graphene in the visible spectrum and demonstrate a hybrid J-aggregate−graphene phototransistor. Until now, J-aggregates have been widely used in demonstration of polariton lasers,[38] solar cells,[39] second harmonic generation,[40] sensitive and selective detection of molecules,[41] nonlinear optical devices,[42] observation of exciton polaritons,[43,44] color selective photodetectors,[45] and synthesis of plexcitonic nanoparticles.[46,47] The recent applications show that J-aggregates could indeed establish a bridge between the fields of photonics and excitonics.[48] However, J-aggregates have not been applied in photodoping of graphene, and thus integration of graphene with J-aggregate family dyes will open new directions for graphene optoelectronics in the visible and near-infrared part of the spectrum.

Owing to the hydrophobicity of polymer transferred single-layer graphene on a surface, it is very challenging to place a polar solvent, i.e., water, soluble quantum dots, or dye molecules on graphene. Previously, to fabricate hybrid light-sensitive gain medium/graphene heterostructure, spin-coating, drop-casting, and supramolecular $\pi-\pi$ stacking[28] have been chiefly used to place molecules and nanomaterials on graphene.[25] It should be noted that although superhydrophilic and superhydrophobic graphene structures in large area can be achieved by vertically aligning graphene nanosheets,[49] single-layer graphene on a flat surface synthesized by chemical vapor deposition and transferred by a polymer, e.g., poly(methyl methacrylate) (PMMA), shows hydrophobic properties, i.e., contact angle of 92°.[50,51] Alternatively, the simple and easy layer-by-layer (LBL) method[52] can be used to create J-aggregate thin films on glass or silicon substrates; however, the method does not work on graphene since aqueous solutions of cationic and anionic polyelectrolytes used in LBL deposition do not properly adhere to the graphene surface.[53] To circumvent this problem, we have developed a new thin film fabrication technique that we call here membrane casting (MC) and successfully fabricated a J-aggregate−graphene phototransistor gated by visible light (Figure 1). Thanks to the hole transfer from J-aggregate thin film to graphene, graphene is effectively p-doped. The new technique enables us to reversibly write and erase charge doping in graphene with visible light. The first integration of graphene with J-aggregate dyes will open new avenues in application of graphene in optoelectronics at visible and near-infrared wavelengths.

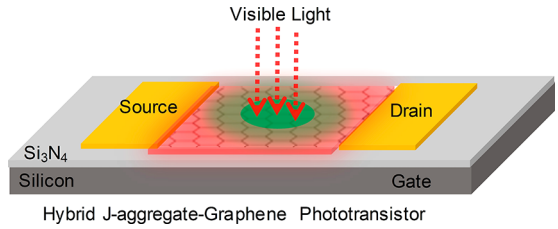

Figure 1. Graphene−J-aggregate hybrid. Schematic representation of the field effect transistor with the excitonic film, i.e., a phototransistor, under visible light illumination. Graphene layer is transferred on Si_3N_4 dielectric film and uniformly covered with excitonic thin film fabricated by the membrane casting technique. The size of the J-aggregate thin film is dictated by the porous polymer membrane. Source and drain electrodes are fabricated by thermal evaporation of gold. The red region between the source and drain represents the J-aggregate sample. Incident photons generate electron−hole pairs in the excitonic film. The holes transfer from J-aggregate thin film to graphene, and hence graphene is effectively p-doped. The charge density on graphene layer is indeed dynamically modulated by the incident photons impinging on the J-aggregate film.

EXPERIMENTAL SECTION

Graphene (typically several cm^2) on copper foils (Mitsui Mining and Smelting Company, Ltd. BI-SBS) was synthesized by the chemical vapor deposition (CVD) technique using methane as a carbon precursor as described in detail previously.[9,54] The copper foils were cut into small pieces and placed on a quartz holder inside a hollow cylindrical quartz tube in a high-temperature furnace. Briefly, the temperature of the growth chamber was first increased to 1035 °C under the flow of 100 sccm H_2 gas flow. Afterward, at 1035 °C, CH_4 gas with 10 sccm flow rate was introduced for a minute. Subsequently, the reaction chamber was cooled to room temperature in about an hour. Afterward, graphene on copper foils was uniformly coated with light-sensitive polymers, i.e., photoresists (Shipley 1813 photoresist), and annealed at 70 °C overnight. Likewise, PMMA can also be used instead of Shipley 1813.[54,55] First, the copper film was completely etched in 1 M $FeCl_3$ aqueous solution. Then, graphene attached to photoresist film was transferred to dielectric substrate by heating first at 80 °C for a few minutes and then at 110 °C for a minute. Finally, the photoresist film was completely removed from graphene by washing with acetone for several times and finally rinsing with isopropyl alcohol. Raman spectra of samples after graphene transfer onto glass and silicon substrates indicate that graphene is indeed single layer in large area.[54] To fabricate flexible graphene devices, graphene was transferred to a 75 μm thick poly(vinyl chloride) substrate by using the hot lamination technique.[54] After etching copper foils, the gold metal electrodes were fabricated. A cyanine dye J-aggregate, (5,5′,6,6′-tetrachlorodi(4-sulfobutyl)benzimidazolocarbocyanine (TDBC), purchased from FEW Chemicals, was used without further purification. To fabricate J-aggregate thin films, a 10 mM TDBC aqueous solution was prepared. In a typical film fabrication, 50 μL of 10 mM TDBC solution was placed between porous polyethylene membrane and a substrate. After 10 min waiting at room temperature, the porous membrane was gently removed from

DOI: 10.1021/acsanm.9b02039
ACS Appl. Nano Mater. 2020, 3, 409−417

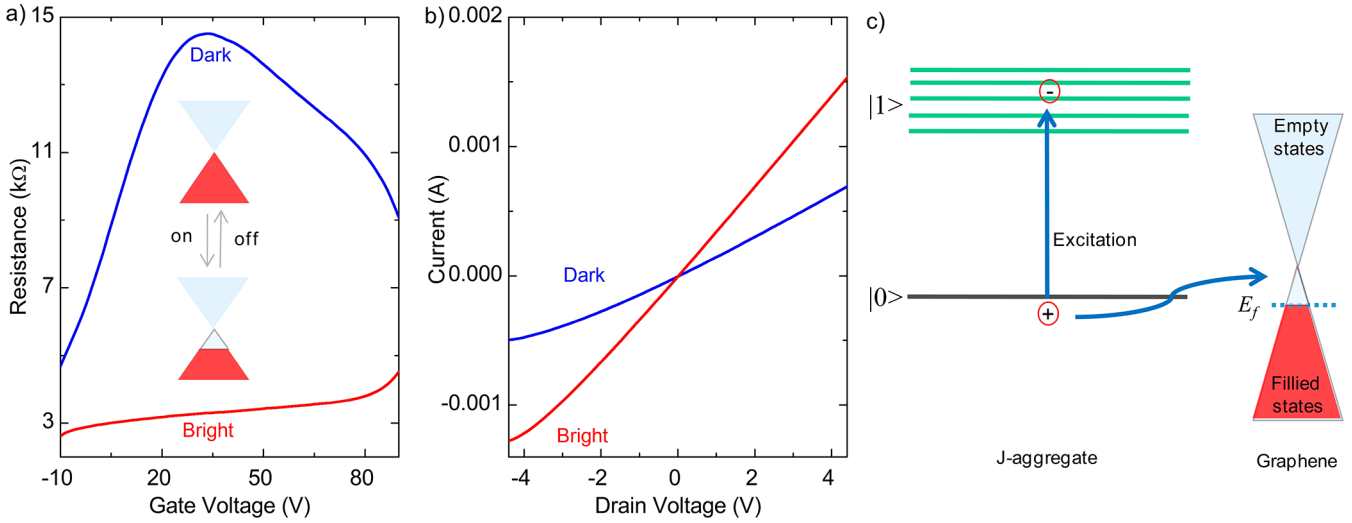

Figure 2. Electrical characterization of hybrid J-aggregate−graphene phototransistor. (a) A graph shows resistance (kΩ) spectra versus applied gate voltages for the bright and dark conditions. Resistance decreases several kiloohms under the visible light illumination because of increase in density of carrier concentration. The Dirac point of graphene can be reversibly tuned by incident photons. (b) Source−drain current as a function of the drain voltage shows increase of the drain current under the visible light illumination. Actually, incident photons generate electron−hole pairs, whereupon holes are transferred to graphene channel. Consequently, holes drift to drain and thus increase the drain current. (c) Schematic representation of the energy level diagram of the J-aggregate−graphene interface. Upon excitation of the J-aggregate, bound states of electrons and holes are created, and subsequently holes are transferred to graphene and electrons are concurrently trapped in the J-aggregate thin film. Eventually, the holes lower the Fermi energy of graphene, and hence, in the bright condition, graphene is heavily hole-doped.

solid J-aggregate film. The porous polyethylene membrane (PEM), which is commonly used as a separator in lithium ion batteries, was purchased from the Gelon LIB Group (Celgard 2730).[56] In fact, the membrane is 20 μm thick and has a porosity of around 43%. Notably, water molecules pass through the pores of the membrane, and an isolated solid J-aggregate thin film was obtained between the porous membrane and substrate. The thickness of the J-aggregate film, measured by a stylus profiler (Dektak-XT, Bruker), is around 150 ± 50 nm. To gate the phototransistor with visible light, a supercontinuum laser (Koheras-SuperK Versa) with acousto-optic tunable filter working in the visible and near-infrared spectra was used as a tunable laser light source with a spectral width of around 1 nm. In addition, the laser beams were expanded and collimated to illuminate the entire surface of the transistor. In reflection and transmission measurements, a variable angle spectroscopic ellipsometer (J. A. Woollam, VASE) was used. The dielectric function of the excitonic thin film was measured by using the same ellipsometer. Photoluminescence (PL) emission measurements of J-aggregate thin films were obtained by using Varian Cary Eclipse fluorescence spectrophotometer. In fact, the excitation wavelengths in PL measurements were varied from 360 to 540 nm with 10 nm increments. While the electrical transport measurements of devices were performed by using a Keithley 2400 source measure unit, the resistance of the J-aggregate/graphene hybrid system was measured by using a Keithley 2000 digital multimeter in an air environment and at room temperature. All electrical and optical measurements were done at ambient conditions.

RESULTS AND DISCUSSION

We fabricated the hybrid graphene−J-aggregate phototransistor and reversibly modulated the Dirac point of graphene. A schematic representation of the phototransistor (i.e., first discovered by John N. Shive in 1949)[57] is shown in Figure 1 where the vertical arrows mark gating of the transistor with visible light, and the current flow between source and drain electrodes is isreversibly altered by the gate voltages. Chemical vapor deposition grown graphene on copper substrates was transferred to silicon substrates for electrical characterization. Notably, Raman measurements have confirmed that graphene on silicon substrate is indeed single layer.[58] An optical microscope (OM) image of a typical large area 2 × 2 cm^2 graphene grown via CVD and transferred on a thick dielectric film is reported in Figure S1a. Source and drain electrodes were fabricated by thermally evaporating 100 nm gold on graphene. It should be noted that graphene on the dielectric film is evidently discernible in the OM image as shown in Figure S1b because of the strong amplitude modulation of reflection at the air−graphene−dielectric interface.[59] The isolated J-aggregate thin film uniformly covers the graphene surface in which the size of the film is veritably determined by the porous membrane size in the MC method (Figure S1b).

Electrical measurements have revealed that graphene can be reversibly doped with incident photons. In the dark condition, the Dirac point of graphene is at around 30 V, which indicates that graphene is indeed hole-doped (Figure 2a). Application of gate voltage to graphene transistor results in accumulation of charge carriers in graphene, and thus the resistance of graphene decreases. In fact, the resistance of the device channel reaches its maximum value at the Dirac point where the carrier concentration is at a minimum. In actuality, we expect to see the Dirac point at around 0 V in undoped graphene, but graphene has an intrinsic hole concentration due to the adsorbates in contact with graphene.[60] Upon illumination with white light, graphene is heavily hole-doped. Notably, there is a large shift in Dirac point of graphene under white light illumination; see the Supporting Information for the spectral distribution of the white-light-emitting diode. Source−drain current measurements show that the hybrid system produces photocurrent when illuminated with white light (Figure 2b). It is evident in the figure that graphene is effectively p-doped under the bright condition. Following absorption of incident photon energies greater than the band gap, J-aggregates on graphene undergo a transition from the ground state to a higher electronic state by generating electron−hole pairs (Frenkel excitons).[48] The absorption of incident photons is

DOI: 10.1021/acsanm.9b02039
ACS Appl. Nano Mater. 2020, 3, 409−417

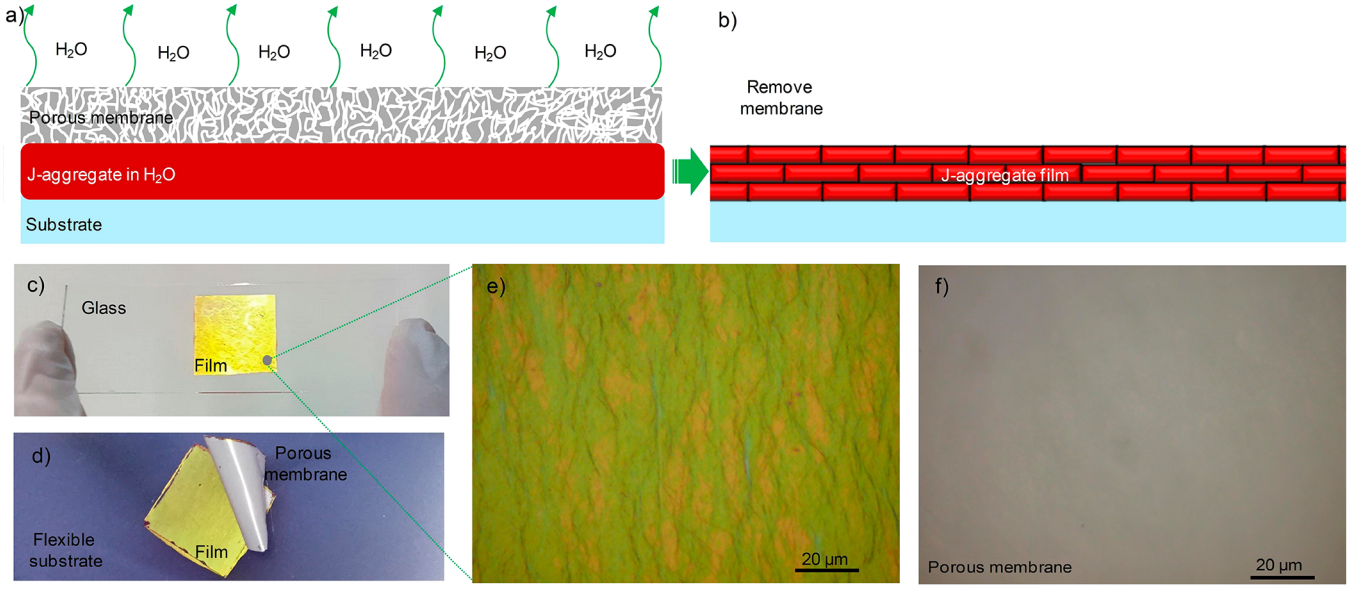

Figure 3. Membrane casting (MC) technique for fabricating J-aggregate thin film. (a) Porous polyethylene membrane assists removal of water molecules from the J-aggregate solution located on a substrate. (b) After removal of the porous membrane, the isolated J-aggregate thin film is yielded on a substrate. It should be noted here that the size of the membrane dictates the final size of the excitonic thin film on the substrate. (c, d, e) Optical microscope images of J-aggregate film on a glass (i.e., a rigid substrate) and poly(vinyl chloride) (i.e., a flexible substrate) indicate uniform film formation. The excitonic film has a golden appearance. (f) Optical microscope images of porous polyethylene membrane. The porous membrane is strongly hydrophobic, and hence the J-aggregate aqueous solution is not allowed to penetrate inside the pores of the membrane.

followed by nonradiative relaxation of excited electrons to lower vibrational states, and then the energy (heat) is released in the process if the electron−hole recombination is radiative (nonradiative).[61] Meanwhile, the holes can also be transferred to graphene, which efficiently dopes graphene and lowers the Fermi level of graphene (Figure 2c). Note that previous observations in PbS quantum dots/graphene hybrids have shown that graphene is p-doped when PbS quantum dots absorb incident photons.[4] In fact, the holes on the graphene channel drift toward the drain and thus increase the drain current while electrons stay in the J-aggregates as it has been also observed in the PbS−graphene system.[4] Therefore, drain current increases in the bright condition. Previously, it was experimentally demonstrated and theoretically calculated that J-aggregates (e.g., TDBC) have exciton diffusion lengths of a few hundred nanometers, which are more than the exciton diffusion lengths measured in typical organic semiconductor and quantum dot films, i.e., around a few tens of nanometers.[62−64] In our case, the J-aggregate film thickness is around 150 ± 50 nm, and hence we can safely assume that most of the generated excitons reach and contribute effective hole doping of the graphene layer. In addition, to understand the effect of excitonic thin film thickness on device performance, we fabricated J-aggregate−graphene hybrids on a flexible substrate (i.e., poly(vinyl chloride) (PVC)) and illuminated the device from the excitonic thin film site (front) and graphene site (back). For optically thick excitonic films we observed only resistance variation from the back-illumination. Therefore, J-aggregate−graphene transistors on transparent substrates can be used in back-illumination to eliminate excitonic film thickness dependence.

The membrane casting (MC) technique has been used to yield J-aggregate thin films on graphene (Figure 3). Briefly, 10 μL of 10 mM TDBC aqueous solution was dropped on a substrate, and the drop was uniformly covered with porous polyethylene membrane as shown in the schematic representation (Figure 3a,b). The substrate and porous membrane strongly adhere to each other because of the capillary forces. Owing to the hydrophobic nature of the membrane,[56] dye solution cannot enter the pores of membrane. Note that dye droplets can be also covered with a glass substrate instead of a porous membrane, but a glass substrate, nevertheless, blocks evaporation of water molecules; hence, in the case of a glass substrate, thin film formation cannot be achieved. After evaporation of water in dye solution, the porous polyethylene membrane is peeled off the rigid and isolated J-aggregate film on a substrate (Figure 3c−f). The force needed to peel an elastic thin film from a substrate has been extensively studied and strongly depends on several parameters such as adhesive surface energy, elastic modulus of the film, and thickness of the film.[65] Recently, based on these parameters, capillary peeling has been proposed and used to detach hydrophobic films from a substrate.[66] Therefore, the interaction between the porous polymer film and J-aggregate on the substrate determines the optical quality of the J-aggregate film. One important advantage of the MC technique over other thin film fabrication techniques is that water-soluble substances can be assembled on virtually all kinds of substrate surfaces, i.e., hydrophilic or hydrophobic, and the size of the film is absolutely dictated by the size of the porous membrane. Thus, the graphene layer is selectively and uniformly coated with an isolated J-aggregate thin film as shown in Figure 3c. In addition, the isolated excitonic thin film does not dissolve in acetone, which means that the excitonic thin film is compatible with lithographic processes (details of the micropattern formation using photolithography will be published elsewhere). In fact, generating an organic superlattice of J-aggregates on a metal substrates is very interesting and attractive, for example, for understanding plexciton mediated energy flow at nanoscale dimension[67] and localization of incident light below the diffraction limit as well.[68]

DOI: 10.1021/acsanm.9b02039
ACS Appl. Nano Mater. 2020, 3, 409−417

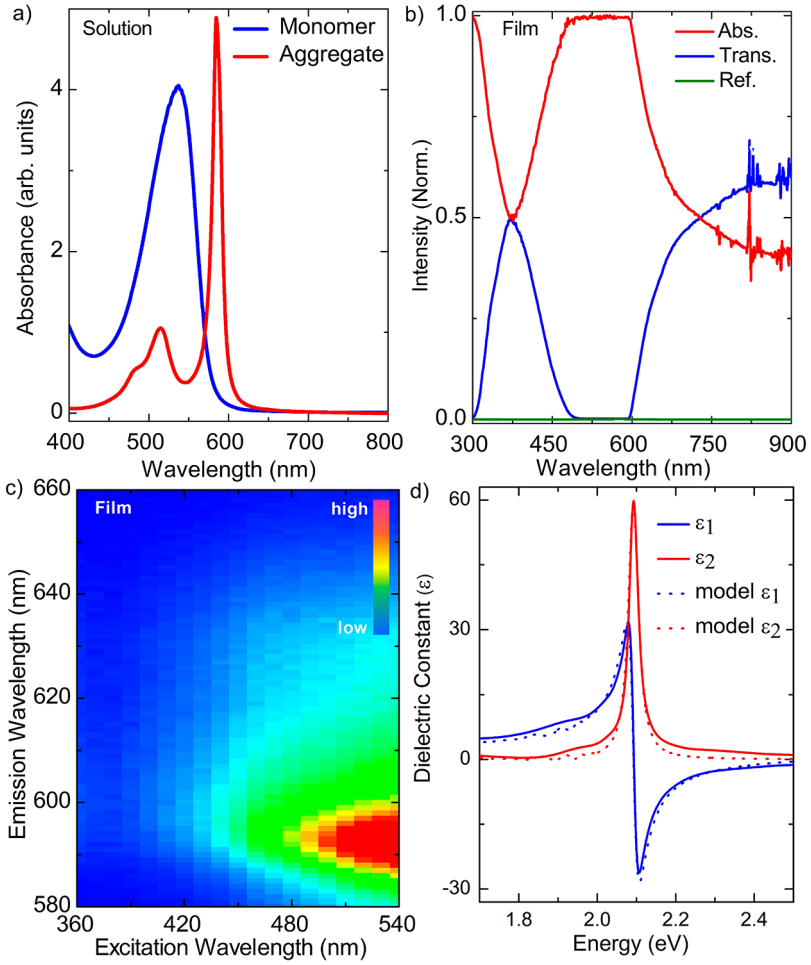

Figure 4. Optical characterization of excitonic thin film. (a) Absorbance spectra of monomer and J-aggregate molecules in water. (b) Transmittance (T), reflectance (R), and absorptance (A) spectra of isolated excitonic thin film fabricated by membrane casting technique ($A + R + T = 1$). (c) Emission of excitonic thin film as a function of excitation wavelength shows broad emission band at around 595 nm. (d) Real (blue line) and imaginary (red line) dielectric constants of isolated J-aggregate thin film measured with an spectroscopic ellipsometer. The results of Lorentz fitting model for real and imaginary dielectric constants are also given.

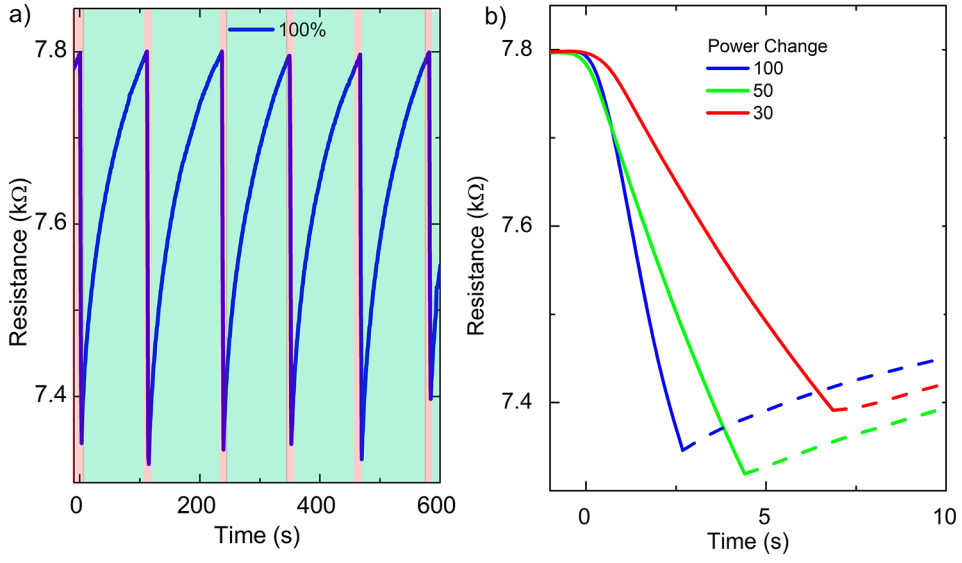

Figure 5. Temporal response of the hybrid J-aggregate/graphene phototransistor in the dark and under illumination. (a) Temporal resistance change of the device at 600 nm and under illumination of 100% power. At full laser power, in less than 3 s about 0.5 kΩ resistance change occurs. Note that the laser is on and off in the red and bright green regions, respectively. (b) Temporal resistance change of the hybrid device as a function of the applied laser power. The dashed lines in the graph indicate when the laser is off.

DOI: 10.1021/acsanm.9b02039
ACS Appl. Nano Mater. 2020, 3, 409−417

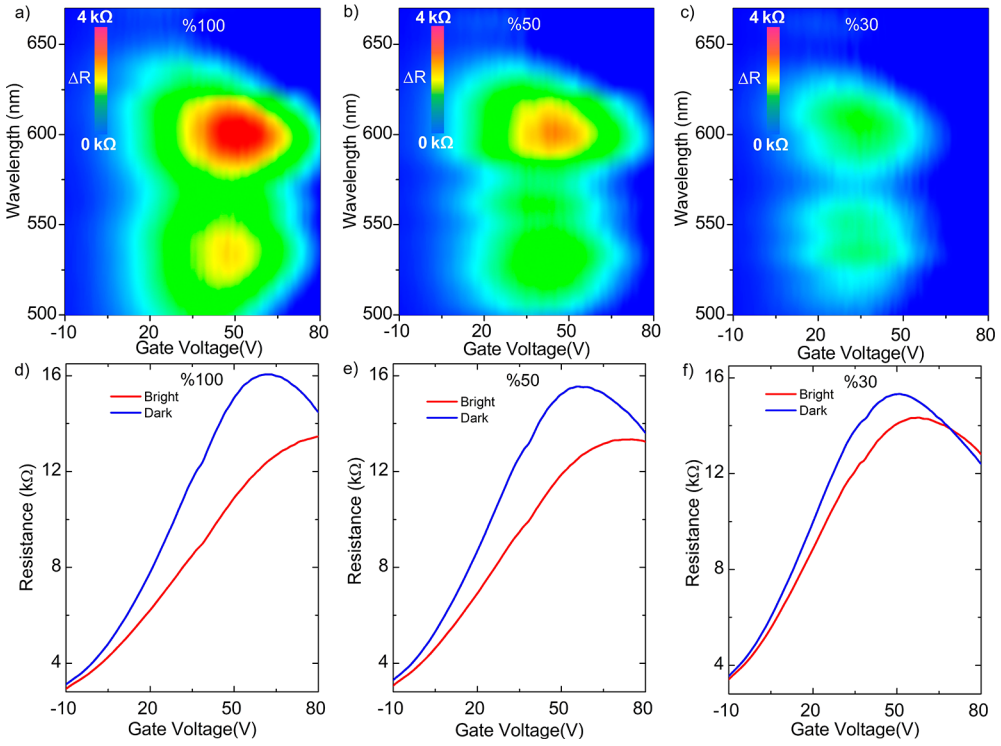

Figure 6. Photoresponse of the phototransistor. (a, b, c) Photoresponse of the phototransistor at (a) 100%, (b) 50%, and (c) 30% laser powers. The red and blue regions indicate large and small resistance variations, respectively. The resistance variation decreases with the applied incident laser power. Along the gate voltage axis, since charge density on graphene changes with the gate voltage, the map is not uniform and represents the location of Dirac point. (d, e) Resistance vs gate voltage graphs show that the Dirac point of graphene can be reversibly tuned with the applied incident laser power at 600 nm. The shift in Dirac point is larger at high laser powers.

Optical characterization of the J-aggregate solution and J-aggregate thin films investigated by using absorption and emission spectroscopy has revealed that J-aggregate thin films and aqueous solutions have very broad and narrow absorbance spectra, respectively, in the visible region while J-aggregates in thin films and in aqueous solution have very similar emission properties (Figure 4). The sharp intense narrow absorption band (~585 nm) at a longer wavelength than monomer peak (~537 nm) is indication of J-aggregate formation in the solution (Figure 4a). The narrow emission peak at around 600 nm dominates the emission map (see the Supporting Information for the emission map). Owing to the aggregation of dye molecules in the J-aggregate thin film, the broad absorbance peak appears in the visible region (Figure 4b). The central emission wavelength of the film is ~595 nm, which is red-shifted with respect to the J-aggregate emission in solution, i.e., ~587 nm (Figure 4c). The real and imaginary dielectric constant of excitonic thin film is shown in Figure 4d. The real part of the dielectric function is negative at high frequencies, and thus exciton polaritons can be generated by using the excitonic thin film.[68]

Now, we would like to examine spectral and power responses of the all-carbon phototransistor by taking a closer look at its measured resistance variation in the dark and under laser light illumination. Temporal resistance variation of the device at 600 nm and 100% laser power as shown in Figure 5a indicates that resistance of graphene can be reversibly tuned by the incident photons. It should be noted that 100% laser power corresponds to 165 μW/cm^2 (see the Supporting Information). At full laser power, in less than 3 s about 0.5 kΩ resistance variation occurs. In fact, the rate of the resistance variation significantly increases with the increase in the incident laser power (Figure 5b). Rise and fall times of the device resistance are not equal to each other, which is most likely due to the surface trap states in J-aggregate−graphene hybrids.[69] Furthermore, the detailed photoresponse of the phototransistor at different laser powers is indicated in Figure 6. The resistance variation decreases with the applied incident laser power. At the Dirac point (at around 40 V gate voltages), the largest resistance variation can be observed (Figure 6a−c). Owing to the variation of the laser power with wavelength (see the Supporting Information), the resistance variation maps in Figure 6a−c are not uniform along the wavelength axis. Along the gate voltage axis, since the charge density on graphene varies with the gate voltage, the resistance variation map is not uniform and represents the location of Dirac point. Indeed, resistance vs gate voltage graphs demonstrate that the Dirac point of graphene can be reversibly tuned with the incident photons. It is obvious in the figure that the shift in Dirac point is larger at high laser powers. The charge density on graphene, which can be deduced from the graphs in Figure 6d−f, increases from 1.5×10^{12} to 4.4×10^{12} cm^{-2} as the incident laser power is tuned from 30% to 100%. The critical parameter indicating the performance of a photodetector is the photoresponsivity R_p, which is expressed as $R_p = \Delta I_p/P_{laser} = (I_{bright} - I_{dark})/P_{laser} = V_{sd}(1/R_{bright} - 1/R_{dark})/P_{laser} = V_{sd}(R_{dark} - R_{bright})/R_{dark}R_{bright}P_{laser}$, where I_p is the photocurrent, P_{laser} is the laser power, and R is the resistance of graphene in the dark and bright conditions, respectively. The responsivity of the phototransistor is calculated to be around ~20 mA/W for the device shown in Figure 6; see the Supporting Information for the laser power dependence of the responsivity.

DOI: 10.1021/acsanm.9b02039
ACS Appl. Nano Mater. 2020, 3, 409−417

CONCLUSION

In conclusion, we have integrated J-aggregate dyes with graphene and demonstrated an all-carbon phototransistor gated by incident photons. We can increase the spectral sensitivity of graphene in the visible spectrum and dynamically tune the Dirac point of graphene in hybrid J-aggregate–graphene structure, and thus the charge density on graphene can be reversibly tuned by visible light. In addition, we have developed a novel, facile thin film fabrication technique we called here as membrane casting (MC) for noncovalent assembly of J-aggregates on graphene. The new thin film fabrication technique allows thin film fabrication of water-soluble nanomaterials and molecules on any surface by using the porous hydrophobic polyethylene membrane. Therefore, MC can be used to fabricate thin films of variety of water-soluble materials such as proteins, metallic or semiconducting nanoparticles, graphene oxide, and polymers on desired substrate surfaces. In the J-aggregate–graphene structure, graphene is very sensitive to the visible light. Graphene is affectively p-doped as confirmed by electrical measurements. Spectral and power responses of the all-carbon phototransistor were measured by using a tunable laser. The first integration of J-aggregates with graphene in a phototransistor fabricated by a new thin film fabrication technique described here enables reversible writing and erasing of charge doping in graphene with incident photons that should prove applicable to a wide range of graphene photonics and optoelectronics applications in the visible and near-infrared region of the electromagnetic spectrum.[1,2]

ASSOCIATED CONTENT

Supporting Information

The Supporting Information is available free of charge at https://pubs.acs.org/doi/10.1021/acsanm.9b02039.

Synthesis and transfer of graphene; membrane casting; phototransistor; Figure S1: the graphene–J-aggregate hybrid; Figure S2: spectral power distribution of laser; Figure S3: spectral and power photoresponse of the phototransistor; Figure S4: thermal chemical vapor deposition system for the synthesis of graphene; Figure S5: membrane casting an aqueous solution of J-aggregates onto flexible substrates; Figure S6: schematic representation of the phototransistor gated by a tunable laser; Figure S7: schematic representation of the phototransistor gated by a white light; Figure S8: emission maps of the dye solution and the excitonic thin film; Figure S9: responsivity (mA/W) of the phototransistor; Figure S10: Raman spectrum of graphene (PDF)

AUTHOR INFORMATION

Corresponding Author

*E-mail: sinanbalci@iyte.edu.tr.

ORCID

Osman Balci: 0000-0003-2766-2197
Burkay Uzlu: 0000-0001-6776-8901
Coskun Kocabas: 0000-0003-0831-5552
Sinan Balci: 0000-0002-9809-8688

Notes

The authors declare no competing financial interest.

ACKNOWLEDGMENTS

This work has been supported by grants (117F172 and 118F066) from the TUBITAK.

REFERENCES

(1) Bonaccorso, F.; Sun, Z.; Hasan, T.; Ferrari, A. C. Graphene photonics and optoelectronics. *Nat. Photonics* **2010**, *4* (9), 611–622.
(2) Avouris, P. Graphene: Electronic and Photonic Properties and Devices. *Nano Lett.* **2010**, *10* (11), 4285–4294.
(3) De Arco, L. G.; Zhang, Y.; Schlenker, C. W.; Ryu, K.; Thompson, M. E.; Zhou, C. W. Continuous, Highly Flexible, and Transparent Graphene Films by Chemical Vapor Deposition for Organic Photovoltaics. *ACS Nano* **2010**, *4* (5), 2865–2873.
(4) Konstantatos, G.; Badioli, M.; Gaudreau, L.; Osmond, J.; Bernechea, M.; de Arquer, F. P. G.; Gatti, F.; Koppens, F. H. L. Hybrid graphene-quantum dot phototransistors with ultrahigh gain. *Nat. Nanotechnol.* **2012**, *7* (6), 363–368.
(5) Koppens, F. H. L.; Mueller, T.; Avouris, P.; Ferrari, A. C.; Vitiello, M. S.; Polini, M. Photodetectors based on graphene, other two-dimensional materials and hybrid systems. *Nat. Nanotechnol.* **2014**, *9* (10), 780–793.
(6) Schuler, S.; Schall, D.; Neumaier, D.; Schwarz, B.; Watanabe, K.; Taniguchi, T.; Mueller, T. Graphene Photodetector Integrated on a Photonic Crystal Defect Waveguide. *ACS Photonics* **2018**, *5* (12), 4758–4763.
(7) Zhang, H.; Tang, D. Y.; Knize, R. J.; Zhao, L. M.; Bao, Q. L.; Loh, K. P. Graphene mode locked, wavelength-tunable, dissipative soliton fiber laser. *Appl. Phys. Lett.* **2010**, *96* (11), 111112.
(8) Sun, Z. P.; Martinez, A.; Wang, F. Optical modulators with 2D layered materials. *Nat. Photonics* **2016**, *10* (4), 227–238.
(9) Salihoglu, O.; Uzlu, H. B.; Yakar, O.; Aas, S.; Balci, O.; Kakenov, N.; Balci, S.; Olcum, S.; Suzer, S.; Kocabas, C. Graphene-Based Adaptive Thermal Camouflage. *Nano Lett.* **2018**, *18* (7), 4541–4548.
(10) Polat, E. O.; Uzlu, H. B.; Balci, O.; Kakenov, N.; Kovalska, E.; Kocabas, C. Graphene-Enabled Optoelectronics on Paper. *ACS Photonics* **2016**, *3* (6), 964–971.
(11) Di, C. A.; Wei, D. C.; Yu, G.; Liu, Y. Q.; Guo, Y. L.; Zhu, D. B. Patterned graphene as source/drain electrodes for bottom-contact organic field-effect transistors. *Adv. Mater.* **2008**, *20* (17), 3289.
(12) Pang, S. P.; Hernandez, Y.; Feng, X. L.; Mullen, K. Graphene as Transparent Electrode Material for Organic Electronics. *Adv. Mater.* **2011**, *23* (25), 2779–2795.
(13) Polat, E. O.; Balci, O.; Kakenov, N.; Uzlu, H. B.; Kocabas, C.; Dahiya, R. Synthesis of Large Area Graphene for High Performance in Flexible Optoelectronic Devices. *Sci. Rep.* **2015**, *5*, 16744.
(14) Wang, Z.; Uzlu, B.; Shaygan, M.; Otto, M.; Ribeiro, M.; Marín, E. G.; Iannaccone, G.; Fiori, G.; Elsayed, M. S.; Negra, R.; Neumaier, D. Flexible One-Dimensional Metal–Insulator–Graphene Diode. *ACS Applied Electronic Materials* **2019**, *1* (6), 945–950.
(15) Uzlu, B.; Wang, Z. X.; Lukas, S.; Otto, M.; Lemme, M. C.; Neumaier, D. Gate-tunable graphene-based Hall sensors on flexible substrates with increased sensitivity. *Sci. Rep.* **2019**, *9*, 18059.
(16) Jariwala, D.; Marks, T. J.; Hersam, M. C. Mixed-dimensional van der Waals heterostructures. *Nat. Mater.* **2017**, *16* (2), 170–181.
(17) Li, J. H.; Niu, L. Y.; Zheng, Z. J.; Yan, F. Photosensitive Graphene Transistors. *Adv. Mater.* **2014**, *26* (31), 5239–5273.
(18) Zeng, L. H.; Wang, M. Z.; Hu, H.; Nie, B.; Yu, Y. Q.; Wu, C. Y.; Wang, L.; Hu, J. G.; Xie, C.; Liang, F. X.; Luo, L. B. Monolayer Graphene/Germanium Schottky Junction As High-Performance Self-Driven Infrared Light Photodetector. *ACS Appl. Mater. Interfaces* **2013**, *5* (19), 9362–9366.
(19) Das, A.; Pisana, S.; Chakraborty, B.; Piscanec, S.; Saha, S. K.; Waghmare, U. V.; Novoselov, K. S.; Krishnamurthy, H. R.; Geim, A. K.; Ferrari, A. C.; Sood, A. K. Monitoring dopants by Raman scattering in an electrochemically top-gated graphene transistor. *Nat. Nanotechnol.* **2008**, *3* (4), 210–215.

DOI: 10.1021/acsanm.9b02039
ACS Appl. Nano Mater. 2020, 3, 409–417

(20) Wang, F.; Zhang, Y. B.; Tian, C. S.; Girit, C.; Zettl, A.; Crommie, M.; Shen, Y. R. Gate-variable optical transitions in graphene. *Science* **2008**, *320* (5873), 206−209.
(21) Zheng, Y.; Ni, G. X.; Toh, C. T.; Tan, C. Y.; Yao, K.; Ozyilmaz, B. Graphene Field-Effect Transistors with Ferroelectric Gating. *Phys. Rev. Lett.* **2010**, *105* (16), 166602.
(22) Schuler, S.; Schall, D.; Neumaier, D.; Dobusch, L.; Bethge, O.; Schwarz, B.; Krall, M.; Mueller, T. Controlled Generation of a p-n Junction in a Waveguide Integrated Graphene Photodetector. *Nano Lett.* **2016**, *16* (11), 7107−7112.
(23) Wei, P.; Liu, N.; Lee, H. R.; Adijanto, E.; Ci, L. J.; Naab, B. D.; Zhong, J. Q.; Park, J.; Chen, W.; Cui, Y.; Bao, Z. A. Tuning the Dirac Point in CVD-Grown Graphene through Solution Processed n-Type Doping with 2-(2-Methoxyphenyl)-1,3-dimethyl-2,3-dihydro-1H-benzoimidazole. *Nano Lett.* **2013**, *13* (5), 1890−1897.
(24) Lee, E. J. H.; Balasubramanian, K.; Weitz, R. T.; Burghard, M.; Kern, K. Contact and edge effects in graphene devices. *Nat. Nanotechnol.* **2008**, *3* (8), 486−490.
(25) Kim, M.; Safron, N. S.; Huang, C. H.; Arnold, M. S.; Gopalan, P. Light-Driven Reversible Modulation of Doping in Graphene. *Nano Lett.* **2012**, *12* (1), 182−187.
(26) Coletti, C.; Riedl, C.; Lee, D. S.; Krauss, B.; Patthey, L.; von Klitzing, K.; Smet, J. H.; Starke, U. Charge neutrality and band-gap tuning of epitaxial graphene on SiC by molecular doping. *Phys. Rev. B: Condens. Matter Mater. Phys.* **2010**, *81* (23), 235401.
(27) Singh, A. K.; Uddin, M. A.; Tolson, J. T.; Maire-Afeli, H.; Sbrockey, N.; Tompa, G. S.; Spencer, M. G.; Vogt, T.; Sudarshan, T. S.; Koley, G. Electrically tunable molecular doping of graphene. *Appl. Phys. Lett.* **2013**, *102* (4), 043101.
(28) Joo, P.; Kim, B. J.; Jeon, E. K.; Cho, J. H.; Kim, B. S. Optical switching of the Dirac point in graphene multilayer field-effect transistors functionalized with spiropyran. *Chem. Commun.* **2012**, *48* (89), 10978−10980.
(29) de Abajo, F. J. G. Graphene Plasmonics: Challenges and Opportunities. *ACS Photonics* **2014**, *1* (3), 135−152.
(30) Ju, L.; Velasco, J.; Huang, E.; Kahn, S.; Nosiglia, C.; Tsai, H. Z.; Yang, W.; Taniguchi, T.; Watanabe, K.; Zhang, Y.; Zhang, G.; Crommie, M.; Zettl, A.; Wang, F. Photoinduced doping in heterostructures of graphene and boron nitride. *Nat. Nanotechnol.* **2014**, *9* (5), 348−352.
(31) Wang, H. I.; Braatz, M. L.; Richter, N.; Tielrooij, K. J.; Mics, Z.; Lu, H.; Weber, N. E.; Mullen, K.; Turchinovich, D.; Klaui, M.; Bonn, M. Reversible Photochemical Control of Doping Levels in Supported Graphene. *J. Phys. Chem. C* **2017**, *121* (7), 4083−4091.
(32) Shao, Y. C.; Liu, Y.; Chen, X. L.; Chen, C.; Sarpkaya, I.; Chen, Z. L.; Fang, Y. J.; Kong, J. M.; Watanabe, K.; Taniguchi, T.; Taylor, A.; Huang, J. S.; Xia, F. N. Stable Graphene-Two-Dimensional Multiphase Perovskite Heterostructure Phototransistors with High Gain. *Nano Lett.* **2017**, *17* (12), 7330−7338.
(33) Lee, Y.; Kwon, J.; Hwang, E.; Ra, C. H.; Yoo, W. J.; Ahn, J. H.; Park, J. H.; Cho, J. H. High-Performance Perovskite-Graphene Hybrid Photodetector. *Adv. Mater.* **2015**, *27* (1), 41−46.
(34) Kobayashi, T. *J-aggregates*; World Scientific: Singapore, 1996; p vii, 228 pp.
(35) Mobius, D. Scheibe Aggregates. *Adv. Mater.* **1995**, *7* (5), 437−444.
(36) Anantharaman, S. B.; Stöferle, T.; Nüesch, F. A.; Mahrt, R. F.; Heier, J. Exciton Dynamics and Effects of Structural Order in Morphology-Controlled J-Aggregate Assemblies. *Adv. Funct. Mater.* **2019**, *29* (21), 1806997.
(37) Kirstein, S.; Mohwald, H. Exciton Band Structures in 2d Aggregates of Cyanine Dyes. *Adv. Mater.* **1995**, *7* (5), 460−463.
(38) Paschos, G. G.; Somaschi, N.; Tsintzos, S. I.; Coles, D.; Bricks, J. L.; Hatzopoulos, Z.; Lidzey, D. G.; Lagoudakis, P. G.; Savvidis, P. G. Hybrid organic-inorganic polariton laser. *Sci. Rep.* **2017**, *7*, 11377.
(39) Sayama, K.; Tsukagoshi, S.; Hara, K.; Ohga, Y.; Shinpou, A.; Abe, Y.; Suga, S.; Arakawa, H. Photoelectrochemical properties of J aggregates of benzothiazole merocyanine dyes on a nanostructured TiO_2 film. *J. Phys. Chem. B* **2002**, *106* (6), 1363−1371.
(40) Schildkraut, J. S.; Penner, T. L.; Willand, C. S.; Ulman, A. Absorption and second-harmonic generation of monomer and aggregate hemicyanine dye in Langmuir−Blodgett films. *Opt. Lett.* **1988**, *13* (2), 134−136.
(41) Liang, W. L.; He, S. H.; Fang, J. Y. Self-Assembly of J-Aggregate Nanotubes and Their Applications for Sensing Dopamine. *Langmuir* **2014**, *30* (3), 805−811.
(42) Yabushita, A.; Fuji, T.; Kobayashi, T. Nonlinear propagation of ultrashort pulses in cyanine dye solution investigated by SHG FROG. *Chem. Phys. Lett.* **2004**, *398* (4−6), 495−499.
(43) Wang, H.; Wang, H. Y.; Bozzola, A.; Toma, A.; Panaro, S.; Raja, W.; Alabastri, A.; Wang, L.; Chen, Q. D.; Xu, H. L.; De Angelis, F.; Sun, H. B.; Zaccaria, R. P. Dynamics of Strong Coupling between J-Aggregates and Surface Plasmon Polaritons in Subwavelength Hole Arrays. *Adv. Funct. Mater.* **2016**, *26* (34), 6198−6205.
(44) Lidzey, D. G.; Bradley, D. D. C.; Armitage, A.; Walker, S.; Skolnick, M. S. Photon-mediated hybridization of Frenkel excitons in organic semiconductor microcavities. *Science* **2000**, *288* (5471), 1620−1623.
(45) Walker, B. J.; Dorn, A.; Bulovic, V.; Bawendi, M. G. Color-Selective Photocurrent Enhancement in Coupled J-Aggregate/Nanowires Formed in Solution. *Nano Lett.* **2011**, *11* (7), 2655−2659.
(46) Balci, S. Ultrastrong plasmon-exciton coupling in metal nanoprisms with J-aggregates. *Opt. Lett.* **2013**, *38* (21), 4498−4501.
(47) Balci, F. M.; Sarisozen, S.; Polat, N.; Balci, S. Colloidal Nanodisk Shaped Plexcitonic Nanoparticles with Large Rabi Splitting Energies. *J. Phys. Chem. C* **2019**, *123*, 26571.
(48) Saikin, S. K.; Eisfeld, A.; Valleau, S.; Aspuru-Guzik, A. Photonics meets excitonics: natural and artificial molecular aggregates. *Nanophotonics* **2013**, *2* (1), 21−38.
(49) Dong, J.; Yao, Z. H.; Yang, T. Z.; Jiang, L. L.; Shen, C. M. Control of Superhydrophilic and Superhydrophobic Graphene Interface. *Sci. Rep.* **2013**, *3*, 1733.
(50) Shin, Y. J.; Wang, Y. Y.; Huang, H.; Kalon, G.; Wee, A. T. S.; Shen, Z. X.; Bhatia, C. S.; Yang, H. Surface-Energy Engineering of Graphene. *Langmuir* **2010**, *26* (6), 3798−3802.
(51) Hong, G.; Han, Y.; Schutzius, T. M.; Wang, Y. M.; Pan, Y.; Hu, M.; Jie, J. S.; Sharma, C. S.; Muller, U.; Poulikakos, D. On the Mechanism of Hydrophilicity of Graphene. *Nano Lett.* **2016**, *16* (7), 4447−4453.
(52) DeLacy, B. G.; Qiu, W. J.; Soljacic, M.; Hsu, C. W.; Miller, O. D.; Johnson, S. G.; Joannopoulos, J. D. Layer-by-layer self-assembly of plexcitonic nanoparticles. *Opt. Express* **2013**, *21* (16), 19103−19112.
(53) Bradley, M. S.; Tischler, J. R.; Bulovic, V. Layer-by-layer J-aggregate thin films with a peak absorption constant of 10(6) cm(−1). *Adv. Mater.* **2005**, *17* (15), 1881.
(54) Balci, O.; Kakenov, N.; Karademir, E.; Balci, S.; Cakmakyapan, S.; Polat, E. O.; Caglayan, H.; Ozbay, E.; Kocabas, C. Electrically switchable metadevices via graphene. *Sci. Adv.* **2018**, *4* (1), eaao1749.
(55) Van Ngoc, H.; Qian, Y.; Han, S. K.; Kang, D. J. PMMA-Etching-Free Transfer of Wafer-scale Chemical Vapor Deposition Two-dimensional Atomic Crystal by a Water Soluble Polyvinyl Alcohol Polymer Method. *Sci. Rep.* **2016**, *6*, 1733.
(56) Arora, P.; Zhang, Z. M. Battery separators. *Chem. Rev.* **2004**, *104* (10), 4419−4462.
(57) Shieve, J. N. Photoreistive translating device. US Patent, 1949.
(58) Ferrari, A. C.; Meyer, J. C.; Scardaci, V.; Casiraghi, C.; Lazzeri, M.; Mauri, F.; Piscanec, S.; Jiang, D.; Novoselov, K. S.; Roth, S.; Geim, A. K. Raman spectrum of graphene and graphene layers. *Phys. Rev. Lett.* **2006**, *97* (18), 187401.
(59) Roddaro, S.; Pingue, P.; Piazza, V.; Pellegrini, V.; Beltram, F. The optical visibility of graphene: Interference colors of ultrathin graphite on SiO_2. *Nano Lett.* **2007**, *7* (9), 2707−2710.
(60) Goniszewski, S.; Adabi, M.; Shaforost, O.; Hanham, S. M.; Hao, L.; Klein, N. Correlation of p-doping in CVD Graphene with Substrate Surface Charges. *Sci. Rep.* **2016**, *6*, 22858.
(61) Akselrod, G. M.; Tischler, Y. R.; Young, E. R.; Nocera, D. G.; Bulovic, V. Exciton-exciton annihilation in organic polariton micro-

DOI: 10.1021/acsanm.9b02039
ACS Appl. Nano Mater. 2020, 3, 409−417

cavities. *Phys. Rev. B: Condens. Matter Mater. Phys.* **2010**, *82* (11), 113106.
(62) Valleau, S.; Saikin, S. K.; Yung, M. H.; Guzik, A. A. Exciton transport in thin-film cyanine dye J-aggregates. *J. Chem. Phys.* **2012**, *137* (3), 034109.
(63) Lunt, R. R.; Giebink, N. C.; Belak, A. A.; Benziger, J. B.; Forrest, S. R. Exciton diffusion lengths of organic semiconductor thin films measured by spectrally resolved photoluminescence quenching. *J. Appl. Phys.* **2009**, *105* (5), 053711.
(64) Lee, E. M. Y.; Tisdale, W. A. Determination of Exciton Diffusion Length by Transient Photoluminescence Quenching and Its Application to Quantum Dot Films. *J. Phys. Chem. C* **2015**, *119* (17), 9005−9015.
(65) Kendall, K. Thin-film peeling-the elastic term. *J. Phys. D: Appl. Phys.* **1975**, *8* (13), 1449.
(66) Khodaparast, S.; Boulogne, F.; Poulard, C.; Stone, H. A. Water-Based Peeling of Thin Hydrophobic Films. *Phys. Rev. Lett.* **2017**, *119* (15), 154502.
(67) Yuen-Zhou, J.; Saikin, S. K.; Zhu, T.; Onbasli, M. C.; Ross, C. A.; Bulovic, V.; Baldo, M. A. Plexciton Dirac points and topological modes. *Nat. Commun.* **2016**, *7*, 11783.
(68) Cacciola, A.; Triolo, C.; Di Stefano, O.; Genco, A.; Mazzeo, M.; Saija, R.; Patane, S.; Savasta, S. Subdiffraction Light Concentration by J-Aggregate Nanostructures. *ACS Photonics* **2015**, *2* (7), 971−979.
(69) Konstantatos, G.; Levina, L.; Fischer, A.; Sargent, E. H. Engineering the temporal response of photoconductive photodetectors via selective introduction of surface trap states. *Nano Lett.* **2008**, *8* (5), 1446−1450.

DOI: 10.1021/acsanm.9b02039
ACS Appl. Nano Mater. 2020, 3, 409−417